JOURNAL OF GEOPHYSICAL RESEARCH, VOL. 100, NO. A11, PAGES 21,623–21,629, NOVEMBER 1, 1995

The whistler-mode bow wave of an asteroid

Donald A. Gurnett

Department of Physics and Astronomy, University of Iowa, Iowa City

Abstract. The Galileo spacecraft has flown by two asteroids, Gaspra in 1990 and Ida in 1993. In both cases the magnetometer detected magnetic field perturbations that are believed to be produced by an interaction of the asteroid with the solar wind. Kivelson et al. have proposed that these perturbations are caused by whistler-mode waves excited by the solar wind flow around the asteroid. This paper presents an analysis of whistler-mode waves generated by the interaction of a small object with the solar wind. Three cases are considered, with the solar wind magnetic field (1) parallel, (2) perpendicular, and (3) at an arbitrary angle to the velocity vector. Using the Cerenkov condition and the quasi-longitudinal approximation for the whistler mode, the angular limits of the wave pattern are determined. For the parallel case the waves are confined to the upstream region, and for the perpendicular case the waves are confined to two wedge-shaped regions extending downstream from the magnetic field line through the object. For intermediate magnetic field orientations the accessibility region maintains the wedge-shaped configuration, with the leading edge of the wedge roughly following the direction of the magnetic field. The outer boundary of the accessibility region is a caustic surface, along which large field amplitudes are expected, similar to the bow wave of a ship. In all cases the interaction involves a characteristic wavelength, $\lambda_c = f_c c^2/(f_p^2 V)$, that is comparable to the size of an asteroid.

1. Introduction

The Galileo spacecraft, which is on its way to Jupiter [*Johnson et al.*, 1992], has flown by two asteroids: Gaspra on October 29, 1990, and Ida on August 28, 1993. During each of these flybys the magnetometer detected magnetic field perturbations that are believed to be caused by an interaction of the asteroid with the solar wind [*Kivelson et al.*, 1993; 1995]. Usually, the magnetic disturbance produced by a large body moving through a magnetized plasma is attributed to Alfven waves generated by the flow around the obstacle. However, asteroids such as Gaspra and Ida are relatively small, with mean diameters of only 14 and 30 km, respectively. These dimensions are much smaller than the mean ion cyclotron radius, which at Gaspra and Ida is approximately 2,000 km. Since Alfven waves require substantial ion motions, *Kivelson et al.* [1993] concluded that such small objects are unlikely to excite Alfven waves. To explain the Galileo observations, Kivelson et al. instead proposed that the magnetic field perturbations are caused by whistler-mode waves. Whistler-mode waves primarily involve the motion of electrons. Since the mean electron cyclotron radius (~1 km) is much smaller than the dimensions of either Gaspra or Ida, Kivelson et al. concluded that these objects should be effective sources of whistler-mode waves.

The purpose of this paper is to carry out an analytic analysis of whistler-mode waves excited by a small object moving through the solar wind. We will show that the Cerenkov condition plays a central role in the interaction. The interaction involves a characteristic wavelength that is comparable to the size of many asteroids. Once generated the waves propagate outward in a characteristic pattern that is controlled by the direction of the solar wind magnetic field. Three cases are considered, with the magnetic field (1) parallel, (2) perpendicular, and (3) at an arbitrary orientation to the velocity vector. The results obtained may be useful for evaluating simulations of asteroid–solar wind interactions, such as those performed by *Wang et al.* [1995]. They may also be useful for interpreting data from future asteroid missions, such as the NEAR spacecraft [*Young*, 1995], which is to rendezvous with the asteroid Eros in 1999.

Paper number 95JA02225.
0148-0227/95/95JA-02225$05.00

2. The Whistler Mode

Before proceeding with the detailed analysis it is useful to summarize some of the relevant characteristics of the whistler mode. The whistler mode is a right-hand polarized electromagnetic mode that propagates at frequencies below the electron cyclotron frequency ω_c and the electron plasma frequency ω_p. Over a wide range of conditions the dispersion relation of the whistler mode can be approximated by the equation

$$\omega(\mathbf{k}) = \frac{c^2 \omega_c}{\omega_p^2} k^2 \cos\theta, \tag{1}$$

where c is the speed of light, k is the wave number, and θ is the angle between the wave vector $\mathbf{k}$ and the magnetic field $\mathbf{B}$. When written in terms of the index of refraction, $n = ck/\omega$, this equation is called the quasi-longitudinal approximation [*Storey*, 1953]. The quasi-longitudinal approximation is valid in the limit of high densities ($\omega_p^2 \gg \omega\omega_c$) and is restricted to a range of frequencies between the ion cyclotron frequency and the electron cyclotron frequency ($\omega_{ci} \lesssim \omega \ll \omega_c \cos\theta$). For a more detailed discussion of the limits of validity of the quasi-longitudinal approximation, see *Helliwell* [1965].

As can be seen from the cos θ term in (1), the whistler mode is highly anisotropic. There are two propagation velocities that must be considered when analyzing the whistler mode: (1) the phase velocity $\mathbf{v}_p$ and (2) the group velocity $\mathbf{v}_g$. The phase

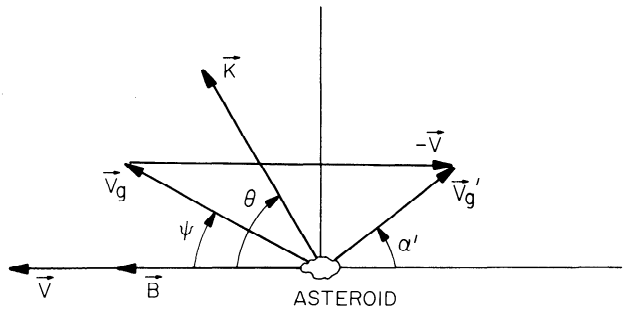

Figure 1. The relevant geometry for the case in which the magnetic field **B** is parallel to the asteroid velocity **V**. The group velocity in the asteroid frame of reference $\mathbf{v}'_g$ is obtained by subtracting the asteroid velocity from the group velocity in the rest frame of the plasma $\mathbf{v}_g$. Anticipating that the wave energy will be swept into the downstream region, the group velocity angle α' is defined relative to the downstream direction.

velocity is the speed at which a condition of constant phase propagates and is in the **k** direction. From (1) it is easy to show that the phase speed ω/k is given by

$$v_p = c \frac{\sqrt{\omega_c \omega}}{\omega_p} \sqrt{\cos \theta}. \tag{2}$$

The group velocity is the velocity of energy propagation [*Stix*, 1962] and is given by $\mathbf{v}_g = \nabla_k \omega(\mathbf{k})$, where ∇_k is a gradient in **k** space and $\omega(\mathbf{k})$ is the dispersion relation. From (1) it is a simple matter to show that the components of the group velocity parallel, $\|$, and perpendicular, $\perp$, to the magnetic field are

$$v_{g\|} = v_p \frac{(1 + \cos^2 \theta)}{\cos \theta}, \tag{3}$$

and

$$v_{g\perp} = v_p \sin \theta. \tag{4}$$

Since the propagation is azimuthally symmetric with respect to the magnetic field, the vectors **k**, $\mathbf{v}_g$, and **B** all lie in the same plane. However, the phase velocity and the group velocity are not at the same angle with respect to the magnetic field. The angle ψ between $\mathbf{v}_g$ and **B** can be obtained by taking the ratio of (4) to (3) and is given by

$$\tan \psi = \frac{\sin \theta \cos \theta}{1 + \cos^2 \theta}. \tag{5}$$

This equation shows that as the wave normal angle θ increases from zero, ψ initially increases, then reaches a maximum $\psi_{max} = \tan^{-1}/(1\sqrt{8}) = 19°28'$ at $\theta_c = \tan^{-1} \sqrt{2} = 57°44'$, and finally decreases back to zero as θ approaches 90°. The upper limit to the angle ψ shows that the whistler mode energy is confined within a cone of directions that makes a half angle of 19°28′ with respect to the magnetic field. This important result was first proven by *Storey* [1953].

3. The Cerenkov Condition

When an object moves at a constant velocity through a dispersive medium, the resulting disturbance can be described by a spectrum of frequencies and wave vectors. However, not all frequencies and wave vectors can be excited. The constraint on ω and **k** is most conveniently illustrated by a delta function source $\delta(\mathbf{r} - \mathbf{V}t)$, where **V** is the velocity of the object relative to the medium. It is straightforward to show that the Fourier transform of this source function is also a delta function, $\delta(\omega - \mathbf{k} \cdot \mathbf{V})$. The frequencies and wave numbers must then satisfy the condition $\omega = \mathbf{k} \cdot \mathbf{V}$. This condition is called the Cerenkov condition. The Cerenkov condition applies to any source geometry, such as a Gaussian or a rectangular distribution, and is a consequence of the uniform motion of the source. The Cerenkov condition appears in many physical situations, such as the radiation from a charged particle moving through a dielectric medium [*Jackson*, 1962]. If we let γ be the angle between **k** and **V**, the Cerenkov condition can be written $\omega = kV \cos \gamma$. It is often useful to express the Cerenkov condition in terms of the phase speed, $v_p = \omega/k$, which becomes

$$v_p = V \cos \gamma. \tag{6}$$

Equation (6) shows that the phase speed of the excited wave must match the projection of the object's velocity onto the wave vector.

Having established the importance of the Cerenkov condition, we are now in a position to analyze the whistler-mode wave pattern generated by the interaction of a uniformly moving object with a magnetized plasma. As the object moves through the plasma, it excites a broad spectrum of frequencies and wave vectors. For any given wave vector the Cerenkov condition (equation (6)) determines the phase speed and frequency of the wave that is excited. The phase speed can then be used in (3) and (4) to compute the group velocity $\mathbf{v}_g$. Note that the group velocity given by these equations is in the plasma frame of reference. The group velocity in the rest frame of the object can be obtained by subtracting the velocity of the object relative to the medium, $\mathbf{v}'_g = \mathbf{v}_g - \mathbf{V}$. By analyzing how $\mathbf{v}'_g$ depends on the wave vector direction, one can then determine the angular limits of the wave pattern and the wavelengths that are excited. This procedure is exactly analogous to the method used to determine the angle of the bow wave excited by a ship moving through deep water. For a discussion of the bow wave of a ship and its relationship to the Cerenkov condition, see *Gurnett* [1995].

4. Magnetic Field Parallel to the Velocity Vector

The case of **B** parallel to **V** is particularly simple and will be treated first. The simplification in this case comes from the fact that the angle θ between **k** and **B** is the same as the angle γ between **k** and **V**. The relevant geometry is shown in Figure 1. Throughout this analysis, **V** will refer to the velocity of the asteroid relative to the solar wind. Since the orbital speed of the asteroid around the Sun is small compared to the solar wind speed, **V** is essentially the negative of the solar wind velocity. Following the procedures outlined in the previous section, the Cerenkov condition (equation (6) with $\gamma = \theta$) is first used to eliminate the phase speed from (3) and (4). The parallel and perpendicular components of the group velocity are then $v_{g\|} = V(1 + \cos^2 \theta)$ and $v_{g\perp} = V \sin \theta \cos \theta$. Note that the plasma parameters, ω_c and ω_p, have completely disappeared from the group velocity. This important simplification occurs independent of the magnetic field orientation and has its roots in the fact that for the quasi-longitudinal approx-

imation the group velocity is always proportional to the phase speed (see (3) and (4)).

Having obtained the group velocity in the plasma frame of reference, the group velocity $\mathbf{v}'_g$ in the asteroid frame of reference can be obtained by subtracting the asteroid velocity, $\mathbf{v}'_g = \mathbf{v}_g - \mathbf{V}$. Anticipating that the waves will be carried downstream, similar to the bow wave of a ship, we define an angle α' between the group velocity $\mathbf{v}'_g$ and the downstream direction (see Figure 1). From the geometry and the above results it is easy to see that this angle is given by

$$\tan \alpha' = -\frac{v'_{g\perp}}{v'_{g\parallel}} = -\frac{V \sin \theta \cos \theta}{V \cos^2 \theta} = -\tan \theta. \qquad (7)$$

Equation (7) has the simple solution $\alpha' = 180° - \theta$. Because of the way α' is defined, i.e., relative to the downstream direction, one can see that the group velocity is parallel to the wave vector. This is a surprising result, given the highly anisotropic nature of the whistler mode. Since the Cerenkov condition can only be satisfied for $\theta \leq 90°$ (angles greater than 90° have negative phase velocities, which violate causality), one can also see that the wave energy must propagate into the upstream region. The region of accessibility is indicated by the shaded region in Figure 2. The wave energy propagates upstream because in the plasma frame of reference the parallel component of the group velocity is always greater than the velocity of the asteroid. Note from (3) that at $\theta = 0°$, $v_g = 2v_p$. This situation is analogous to capillary waves in water, which produce a wave pattern upstream of an obstacle because the group velocity is greater than the phase velocity [*Segel*, 1987]. It is also interesting to note that over the entire range of allowed propagation angles, there is no angle at which $\partial\alpha'/\partial\theta = 0$. In optics the condition $\partial\alpha'/\partial\theta = 0$ is called a caustic focus. At a caustic focus a large number of waves are focused into a small range of angles, thereby greatly increasing the wave intensity. The bow wave of a ship is a caustic focus (see the discussion by *Gurnett* [1995]). Thus for the parallel case the upstream wave pattern does not have a bow wave analogous to the bow wave of a ship. The wave intensity simply decays with increasing distance from the asteroid, varying roughly as $1/r^2$, where r is the distance from the asteroid.

Before closing the discussion of the parallel case it is of interest to compute the wavelength λ of the waves generated by the interaction. The wave number, $k = 2\pi/\lambda$, can be obtained by using the Cerenkov condition ($\omega = kV \cos \gamma$, with $\gamma = \theta$) to eliminate the frequency from the dispersion relation (equation (1)). When this is done, it is evident that the cos θ term cancels on both sides of the equation. The wave number is then constant, independent of the wave normal angle, and is given by

$$k_c = \frac{\omega_p^2 V}{\omega_c c^2}. \qquad (8)$$

The corresponding wavelength is $\lambda_c = f_c c^2/(f_p^2 V)$. Using the approximate parameters for the Gaspra flyby [*Kivelson et al.*, 1993], $f_p = 10$ kHz, $f_c = 50$ Hz, and $V = 400$ km/s, the characteristic wavelength is $\lambda_c = 112$ km. The size scale, $\lambda_c/2\pi$, that would be most effective for exciting this wavelength is approximately 18 km. This scale size is comparable to the size of the Gaspra and Ida, as well as many other asteroids. Thus these objects have the proper scale size to be effective sources of whistler-mode waves.

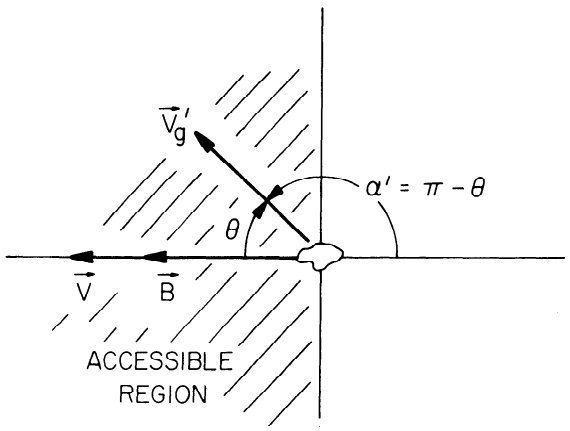

Figure 2. Contrary to what one might expect, for the parallel case, all of the wave energy propagates into the upstream region. This occurs because the parallel component of the group velocity in the plasma rest frame is always greater than the asteroid velocity.

5. Magnetic Field Perpendicular to the Velocity Vector

The case where the magnetic field is perpendicular to the velocity vector is more complicated but is more realistic, since the solar wind magnetic field tends to make a large angle with respect to the solar wind velocity beyond about 1 AU. The relevant geometry is illustrated in Figure 3. Because the geometry is inherently three dimensional, it is useful to carry out the analysis in a plane containing **V** but rotated at an angle δ relative to the **B**, **V** plane. This plane is labeled the "analysis plane" in Figure 3. Assume that we start with a wave vector **k** that makes an angle θ with respect to the magnetic field. The group velocity of this wave (in the plasma rest frame) then lies on a cone that makes an angle ψ with respect to the magnetic field, where ψ is given by (5). This cone is labeled "group velocity cone" in Figure 3. The group velocity cone intersects the analysis plane at the two azimuthal angles indicated by the solid circles at the top of the cone. Only the forward solution, labeled $\mathbf{v}_g$, need be considered, since the rearward solution violates causality (i.e., $v_p = V \cos \gamma$ is negative). From (5) and the basic geometry it is easy to show that the azimuthal angle ϕ is given by

$$\sin \phi = \frac{(1 + \cos^2 \theta)}{\sin \theta \cos \theta} \tan \delta. \qquad (9)$$

This equation has no solution if the angle δ is greater than $\delta_{max} = \tan^{-1}(1/\sqrt{8}) = 19°28'$. Thus no wave energy can exist outside of a wedge-shaped region that makes an angle of more than 19°28′ from the **B**, **V** plane. Since **B**, $\mathbf{v}_g$, and **k** all lie in the same plane (indicated by the dashed rectangle in Figure 3), the azimuthal angle ϕ of the **k** vector is the same as the azimuthal angle ϕ of the group velocity. Having determined θ and ϕ, we can compute γ, the angle between **k** and **V**. This angle is given by $\cos \gamma = \sin \theta \cos \phi$. The Cerenkov condition (see (6)) then becomes

$$v_p = V \sin \theta \cos \phi. \qquad (10)$$

Using (10), the phase speed can be eliminated from (3) and (4). The perpendicular and parallel components of the group velocity are then given by $v_{g\perp} = V \sin^2 \theta \cos \phi$ and $v_{g\parallel} =$

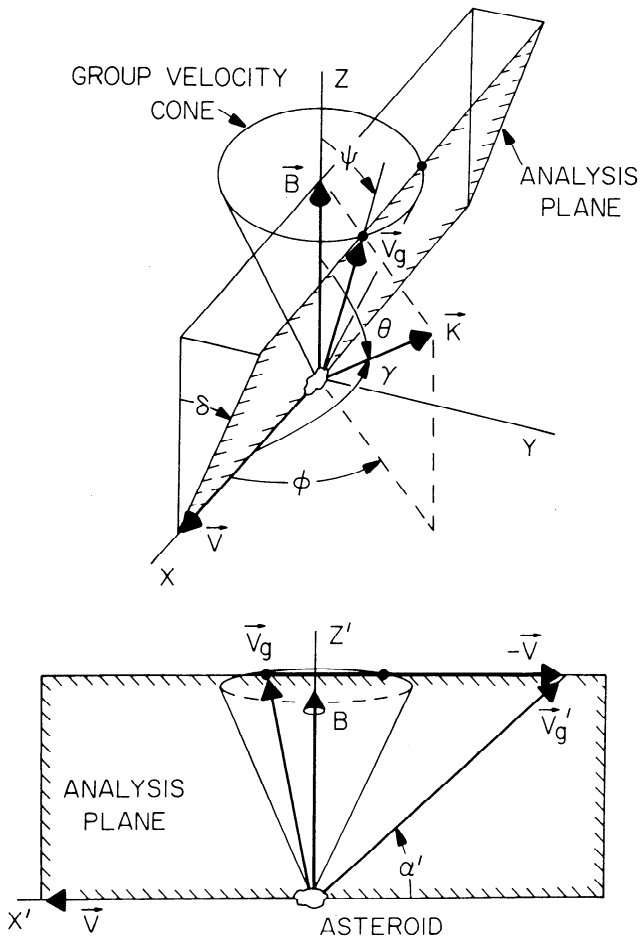

Figure 3. The relevant geometry for the case in which the magnetic field **B** is perpendicular to the asteroid velocity **V**. The analysis is most conveniently performed in a plane tilted at an angle δ relative to the **B**, **V** plane. Again, the group velocity angle α' is defined relative to the downstream direction.

$V(1 + \cos^2\theta) \tan\theta \cos\phi$. Just as in the parallel case, the plasma parameters, ω_c and ω_p, have completely disappeared from the group velocity.

Having obtained the group velocity in the plasma frame of reference, it is now a simple matter to compute the group velocity in the asteroid frame of reference by subtracting the velocity of the asteroid relative to the plasma, $\mathbf{v}'_g = \mathbf{v}_g - \mathbf{V}$. This calculation is best done in a x', z' coordinate system that lies in the analysis plane (see Figure 3). The corresponding components of the group velocity in this frame of reference are $v'_{gz'} = V[(1 + \cos^2\theta)\tan\theta\cos\phi\cos\delta + \sin^2\theta\cos\phi\sin\phi\sin\delta]$ and $v'_{gz'} = -V(1 - \sin^2\theta\cos^2\phi)$. From these group velocity components one can then determine the angle α' between the group velocity and the downstream direction (see Figure 3). This angle is given by

$$\tan\alpha' = \frac{(1 + \cos^2\theta)\tan\theta\cos\phi\cos\delta + \sin^2\theta\cos\phi\sin\phi\sin\delta}{1 - \sin^2\theta\cos^2\phi} \quad (11)$$

Note that α' is completely independent of the physical parameters of the problem. As in the parallel case this simplification is a direct consequence of the fact that for the quasi-longitudinal approximation the group velocity is proportional to the phase speed.

To explore the angular limits of the wave pattern, we can now use (11) to plot the group velocity direction α' as a function of the wave normal angle θ. A plot of α' versus θ for various values of δ is shown in the top panel of Figure 4, along with a similar plot of ϕ versus θ in the bottom panel. As can be seen, solutions for α' exist only over a limited range of θ values. As δ increases, the range of allowed θ values decreases. This trend is a direct consequence of the upper limit, $\psi_{max} = 19°28'$, on the group velocity direction relative to the magnetic field. No solution exists for δ greater than $\delta_{max} = 19°28'$. Within the range of allowed δ values the solution always begins and ends at $\phi = 90°$, corresponding to θ values for which the group velocity cone is just tangent to the analysis plane (see Figure 3). As θ increases, α' increases from zero, reaches a maximum α'_{max}, and then decreases back to zero. The existence of an upper limit to the group velocity angle means that all of the wave energy is directed downstream into a V-shaped region, similar to the bow wave of a ship. Since this upper limit is a caustic focus, $\partial\alpha'/\partial\theta = 0$, the largest wave amplitudes should

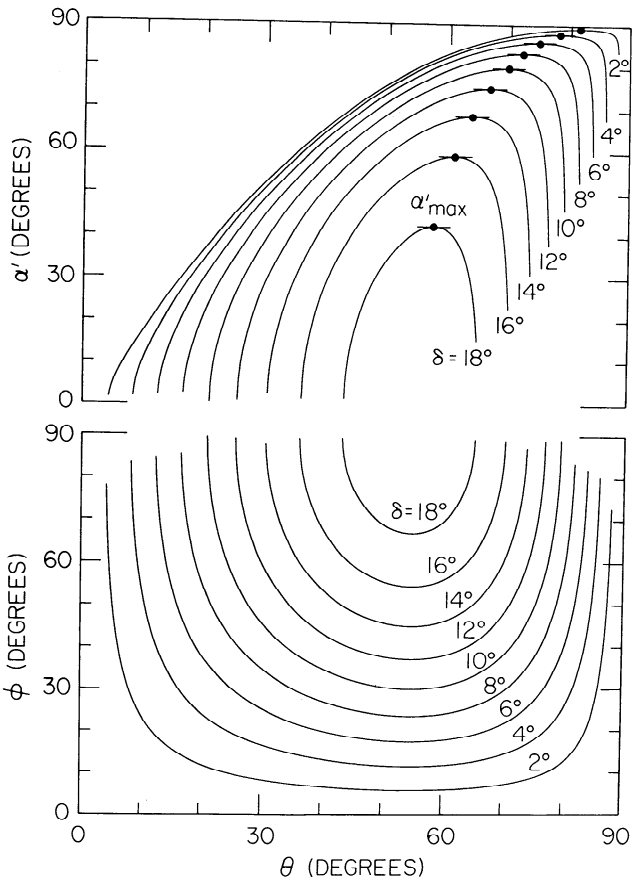

Figure 4. (top) The group velocity direction α' as a function of the wave normal angle θ and (bottom) the azimuthal angle ϕ of the wave vector as a function of θ. The existence of a maximum, α'_{max}, in the group velocity direction shows that the wave energy is directed into a V-shaped region downstream of the asteroid, similar to the bow wave of a ship. The angle α'_{max} increases as the angle δ of the analysis plane decreases. No solution exists for $|\delta| > 19°28'$.

also occur along this V-shaped boundary. As the angle δ of the analysis plane varies from 0 to $\delta_{max} = 19°28'$, the bow wave angle α'_{max} varies smoothly from 90° to 0°.

Before closing the discussion of the perpendicular case it is of interest to examine the wavelengths generated by the interaction. As with the parallel case the wave number is obtained by using the Cerenkov condition, $\omega = kV \sin\theta \cos\phi$ (from (10)), to eliminate the frequency from the dispersion relation (equation (1)). The result is

$$k = k_c \tan\theta \cos\phi, \tag{12}$$

where k_c is the characteristic wave number defined earlier (equation (8)). A plot of k/k_c as a function of θ is shown in Figure 5 for various values of δ. The solid circle on each curve corresponds to the point at which α'_{max} occurs in Figure 4. Since these points correspond to the angles where the maximum intensities occur (i.e., the caustic focus), they are the wave numbers of primary interest. As can be seen, these wave numbers lie in the range from about $k/k_c \sim 0.5$ to 5. For Gaspra the corresponding wavelengths range from about 20 to 200 km. The scale sizes required to provide optimal excitation are again comparable to the dimensions of Gaspra and Ida, as well as many other asteroids.

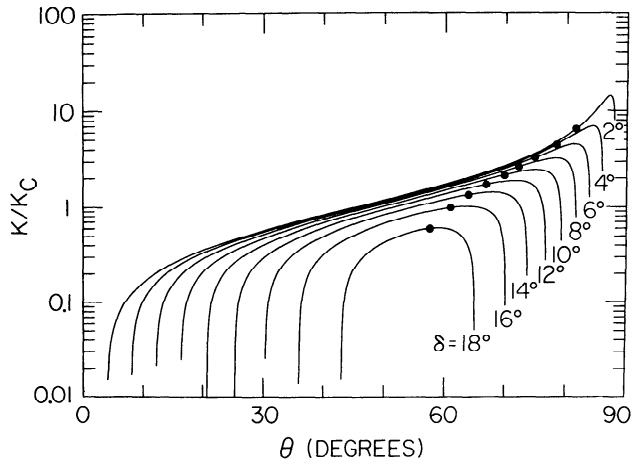

Figure 5. A plot of the ratio of the wave number to the characteristic wave number, k/k_c, as a function of the wave normal angle θ. The solid circles correspond to the points where $\partial\alpha'/\partial\theta = 0$ in Figure 4. These are the points where the maximum wave intensity is expected to occur.

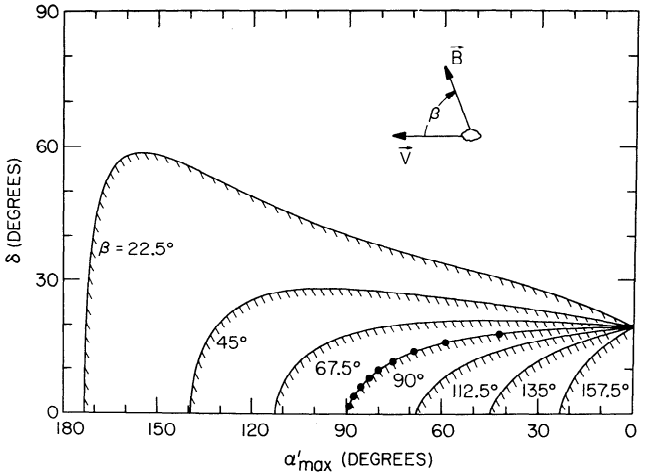

Figure 6. A plot of α'_{max} as a function of δ for various magnetic field orientations. These curves give the outer accessibility limits for whistler-mode waves excited by the asteroid. They also are caustic surfaces, $\partial\alpha'/\partial\theta = 0$, along which the largest wave intensities are expected to occur (similar to the bow wave of a ship).

6. Arbitrary Magnetic Field Orientation

The analysis of the whistler-mode waves excited for an arbitrary magnetic field orientation is qualitatively similar to the perpendicular case but involves additional geometric complexities. Because of these complexities we will only summarize the essential results. From Figure 3 one can see that if the magnetic field is tipped forward, toward the velocity vector, then both solutions for the group velocity must be considered. If β is the angle between **V** and **B**, it can be shown that the azimuthal angle ϕ (in a plane perpendicular to **B**, measured positive in the right-hand sense from the forward half of the x-y plane) is given by

$$\cos\phi = \frac{-M \pm N\sqrt{N^2 + M^2 - 1}}{(M^2 + N^2)}, \tag{13}$$

where $M = -\tan\psi/\tan\beta$ and $N = \tan\psi/(\tan\delta \sin\beta)$. The angle γ between the wave vector **k** and the velocity vector **V** is then given by

$$\cos\gamma = \sin\theta\cos\phi\sin\beta + \cos\theta\cos\beta. \tag{14}$$

For $0 \le \beta \le 90°$, both signs in (13) must be used. However, only those ϕ values that give $\cos\gamma \ge 0$ can be used, since the causality condition is only satisfied for wave vectors in the forward hemisphere. For $90° < \beta \le 180°$ the minus sign always gives $\cos\gamma < 0$, so only the plus sign need be considered.

By using appropriate coordinate rotations and transformations it can be shown that the group velocity direction α' in the analysis plane is given by

$$\begin{aligned}\tan\alpha' = {} & \{\sin\theta\cos\gamma(\sin\phi\sin\delta - \cos\phi\cos\beta\cos\delta) \\ & + [(1 + \cos^2\theta)/\cos\theta]\cos\gamma\sin\beta\cos\delta\} \\ & \cdot\{1 - \sin\theta\cos\gamma\cos\phi\sin\beta \\ & - [(1 + \cos^2\theta)/\cos\theta]\cos\gamma\cos\beta\}^{-1},\end{aligned} \tag{15}$$

It is easy to show that (15) reduces to the same results obtained for the parallel case if $\beta = 0$ and for the parallel case if $\beta = 90°$. Using (15), plots of α' versus θ can be constructed similar to Figure 4. From these plots the maximum group velocity angle α'_{max} can be determined as a function of the angle δ. A plot of α'_{max} versus δ is shown in Figure 6 for various magnetic field orientations. The solid circles on the $\beta = 90°$ curve correspond to the perpendicular case shown in the top panel of Figure 4. The curves are an even function of δ, i.e., $\alpha'(-\delta) = \alpha'(\delta)$. For $\beta = 90°$ one can see that the α'_{max} versus δ curves generate two smooth wedge-shaped surfaces of the type shown in Figure 7, one facing upward and the other facing downward. Since α'_{max} is defined by $\partial\alpha'/\partial\theta = 0$, these surfaces are caustic surfaces. They also represent the accessibility limit of the excited wave pattern. All the excited waves must lie within these surfaces. From the β dependence one can see that as the magnetic field is tipped forward from perpendicular (toward **V**), the upward facing accessibility region tips forward, and the downward fac-

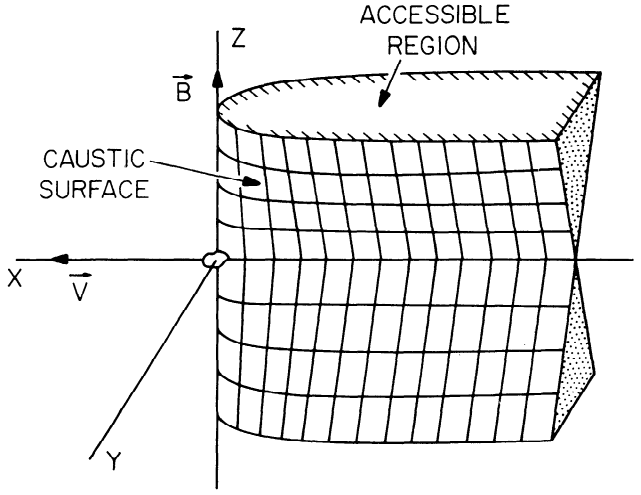

Figure 7. For the case in which **B** is perpendicular to **V** the wave energy is confined to two wedge-shaped surfaces that extend downstream from the magnetic line through the asteroid. The shape of this surface is determined by plotting α'_{max} as a function of δ (see Figures 4 and 6).

ing accessibility region tips backward. As the magnetic field direction approaches $\beta = 0°$, the upward (forward) facing accessibility region expands and maps into the entire forward hemisphere as **B** becomes parallel to **V**. Meanwhile, the downward (backward) facing accessibility region shrinks to zero ($\alpha'_{max} = 0$) as **B** becomes parallel to **V**. In the far downstream direction the accessibility surface acquires a wedge-shaped configuration consisting of two planes that are at angles of $\delta_{max} = \pm 19°28'$ to the **B**, **V** plane.

7. Conclusion

In this paper we have examined the generation of whistler-mode waves by the interaction of an asteroid with the solar wind. An interaction of this type is believed to have been responsible for the magnetic field perturbations observed during the Galileo flybys of the asteroids Gaspra and Ida. A fundamental feature of this interaction is the Cerenkov condition, which determines the phase speed of the emitted waves in the rest frame of the plasma. By combining the Cerenkov condition with the quasi-longitudinal approximation for the whistler mode, we have obtained an analytical solution for the direction of energy propagation (group velocity). These solutions were then used to determine the angular limits of the emitted wave pattern in the asteroid frame of reference for three cases, with the magnetic field (1) parallel, (2) perpendicular, and (3) at an arbitrary angle to the velocity vector. In the parallel case the waves were found to be constrained entirely to the upstream region. This occurs because in the rest frame of the plasma the parallel component of the group velocity is always greater than the asteroid velocity. In the perpendicular case the emitted waves were found to be confined to two wedge-shaped regions extending downstream from the magnetic field line through the asteroid. Because of wave focusing effects, large wave intensities are expected along the boundary of this wedge-shaped region, very similar to the bow wave of a ship. For an arbitrary magnetic field orientation we showed that as the magnetic field is tipped forward from perpendicular (toward **V**), the upward facing accessibility region tips forward, and the downward facing accessibility region tips backward. As **B** becomes parallel to **V**, the upward (forward) facing region expands and eventually maps into the entire forward hemisphere. Meanwhile, the downward (backward) facing region shrinks to zero. The backward facing accessibility region disappears when **B** is parallel to **V** because the causality condition cannot be satisfied for wave vector directions in the backward facing hemisphere (i.e., γ must be less than 90° in (6)). In all cases the wavelengths excited are determined by a characteristic wave number $k_c = \omega_p^2 V/(\omega_c c^2)$. For typical solar wind parameters the scale lengths required to excite these waves are comparable to the dimensions of many moderate-sized asteroids.

Before finishing the discussion we must consider the extent to which the quasi-longitudinal approximation is satisfied. There are two requirements that must be met. First, the plasma density must be sufficiently high to satisfy the condition $f_p^2 \gg ff_c$. Second, the frequency in the rest frame of the plasma must be in the range $f_{ci} \lesssim f \ll f_c \cos\theta$. To evaluate the rest frame frequency, we first consider the parallel case with $\theta = 0°$. For $\theta = 0°$ the rest frame frequency is given by $f = V/\lambda_c$, where λ_c is the characteristic wavelength given by (8). Using the representative parameters for Gaspra, $f_p = 10$ kHz, $f_c = 50$ Hz, $V = 400$ km/s, and $\lambda_c = 112$ kHz, the rest frame frequency is $f = 3.6$ Hz. Using this frequency, it is easy to verify that the density condition, $f_p^2 \gg ff_c$, is satisfied by a large factor. The rest frame frequency is also well above the ion cyclotron frequency, $f_{ci} \simeq 0.03$ Hz, and well below the electron cyclotron frequency, $f_c = 50$ Hz, so the condition $f_{ci} \lesssim f \ll f_c$ is also satisfied. As the wave normal direction increases from $\theta = 0°$, the rest frame frequency decreases, varying as $\cos\theta$. This variation occurs because of the $\cos\gamma$ term in the Cerenkov condition (for the parallel case $\gamma = \theta$). Because the rest frame frequency varies as $\cos\theta$, the upper limit in the condition $f_{ci} \lesssim f \ll f_c \cos\theta$ remains satisfied for all wave normal angles. However, the lower limit is violated but only at very large wave normal angles, of the order of 89°. Thus in the parallel case the quasi-longitudinal approximation is valid over almost the entire region of physical interest.

For the perpendicular case the validity of the quasi-longitudinal approximation is more difficult to evaluate because of the numerous angular dependences. These mainly involve the $\tan\theta\cos\phi$ terms in (12) and the $\cos\gamma$ term in the Cerenkov condition. Since the largest wave amplitudes are expected near the caustic points, $\partial\alpha'/\partial\theta = 0$, we will concentrate on the parameters in the vicinity of the circles in Figures 4 and 5. At a representative point, for example, $\theta = 64°$ and $\delta = 14°$ in Figure 4 (for which $\phi = 50°$, $\gamma = 55°$, and $k/k_c = 1.3$), it is easily verified that the condition $f_{ci} \lesssim f \ll f_c \cos\theta$ is satisfied by a comfortable margin ($f = 2.8$ Hz and $f_c \cos\theta = 22$ Hz). As the wave normal angle increases, the upper limit eventually becomes compromised at wave normal angles of the order of 80 to 85°. This is due to the fact that k/k_c increase rapidly, which raises the rest frame frequency. Thus the validity of the solution is compromised in a narrow region around $\alpha' \simeq 90°$ (i.e., along the magnetic field line in Figure 5). Except for this narrow region the quasi-longitudinal approximation is satisfied over the entire region of physical interest. Similar conclusions also apply for magnetic field orientations between the parallel and perpendicular cases.

Various improvements in this model could no doubt be considered. The failure of the quasi-longitudinal approximation at large wave normal angles could be repaired by using the equation

$$n^2 = \frac{\omega_p^2}{\omega(\omega_c \cos \theta - \omega)}, \quad (16)$$

which gives a better approximation for the index of refraction at large wave normal angles [see *Helliwell*, 1965]. Unfortunately, for this equation the group velocity is no longer proportional to the phase speed at all wave normal angles, which was a key simplifying element in the preceding analysis. Whether the analysis can be reformulated using (13) remains to be investigated. It is also possible that Landau damping and cyclotron damping could become significant factors for large wave normal angles and for frequencies near the electron cyclotron frequency. Wave damping would, of course, limit the range at which significant perturbations could be observed.

Acknowledgments. The author wishes to thank Scott Allendorf for his help in making various plots used in this paper. This research has been supported by the Jet Propulsion Laboratory under contract 958779.

The Editor thanks Z. Wang and U. S. Inan for their assistance in evaluating this paper.

References

Gurnett, D. A., On a remarkable similarity between the propagation of whistlers and the bow wave of a ship, *Geophys. Res. Lett.*, *22*, 1865–1868, 1995.

Helliwell, R. A., *Whistlers and Related Ionospheric Phenomena*, pp. 23–31, Stanford Univ. Press, Stanford, Calif., 1965.

Jackson, J. D., *Classical Electrodynamics*, p. 494, John Wiley, New York, 1962.

Johnson, T. V., C. M. Yeates, and R. Young, Space Science Reviews volume on the Galileo mission, *Space Sci. Rev.*, *60*, 3–21, 1992.

Kivelson, M. G., L. F. Bargatze, K. K. Khurana, D. J. Southwood, R. J. Walker, and P. J. Coleman Jr., Magnetic field signatures near Galileo's closest approach to Gaspra, *Science*, *261*, 331–334, 1993.

Kivelson, M. G., Z. Wang, S. Joy, K. K. Khurana, C. Polansky, D. J. Southwood, and R. J. Walker, Solar wind interaction with small bodies, 2, What can Galileo's detection of magnetic rotations tell us about Gaspra and Ida, *Adv. Space Sci.*, *16*(4), 59–68, 1995.

Segel, L. A., *Mathematics Applied to Continuum Mechanics*, p. 409, Dover, Mineola, N. Y., 1987.

Stix, T. H., *The Theory of Plasma Waves*, p. 52, McGraw-Hill, New York, 1962.

Storey, L. R. O., An investigation of whistling atmospherics, *Philos. Trans. R. Soc. London A*, *246*, 113–141, 1953.

Wang, Z., M. G. Kivelson, S. Joy, K. K. Khurana, C. Polansky, D. J. Southwood, and R. J. Walker, Solar wind interaction with small bodies, 1, Whistler wing signatures near Galileo's closest approach to Gaspra and Ida, *Adv. Space Sci.*, *16*(4), 47–57, 1995.

Young, L., Near spacecraft ahead of schedule, *APL News*, *51*(2), 1, 1995.

D. A. Gurnett, Department of Physics and Astronomy, University of Iowa, Van Allen Hall, Iowa City, IA 52242. (e-mail: gurnett@iowave.physics.uiowa.edu)

(Received February 24, 1995; revised June 1, 1995; accepted July 19, 1995.)